RESEARCH PAPER

ANALYSIS OF THE MANGROVE STRUCTURE IN THE DONG RUI COMMUNE BASED ON MULTISPECTRAL UNMANNED AERIAL VEHICLE IMAGE DATA

Dung Trung Ngo[1,*], Khanh Nguyen Quoc[1], Ngoc Thi Dang[2], Cuong Hung Dang[1], Lan Linh Tran[3] and Hoi Dang Nguyen[1,*]

[1]Institute of Tropical Ecology, Joint Vietnam-Russia Tropical Science and Technology Research Center, № 63, Nguyen Van Huyen Str., Cau Giay District, Hanoi, Vietnam.

[2]University of Science, Vietnam National University, No. 334, Nguyen Trai Str., Thanh Xuan District, Hanoi, Vietnam.

[3]Quang Ninh Department of Natural Resources and Environment, W4VF+P3 V, Nguyen Van Cu Str., Ha Long District, Quang Ninh, Vietnam.

***Corresponding author:** ngotrungdung266@gmail.com, danghoi110@gmail.com

Received: November 20th, 2022 / Accepted: November 14th, 2023 / Published: December 31st, 2023

https://DOI-10.24057/2071-9388-2023-2641

ABSTRACT. Mangroves are one of the most important types of wetlands in coastal areas and perform many different functions. Assessing the structure and function of mangroves is a premise for the management, monitoring and development of this most diverse and vulnerable ecosystem. In this study, the unmanned aerial vehicle (UAV) Phantom 4 Multispectral was used to analyse the structure of a mangrove forest area of approximately 50 hectares in Dong Rui commune, Tien Yen district, Quang Ninh Province – one of the most diverse wetland ecosystems in northern Vietnam. Based on the visual classification method combined with the results of field taxonomic sampling, a mangrove tree classification map was established for UAV with three species, *Bruguiera gymnorrhiza, Rhizophora stylosa,* and *Kandelia obovata*, achieving an overall accuracy = 86.28%, corresponding to a Kappa coefficient =0.84. From the images obtained from the UAV, we estimated and developed maps and assessed the difference in tree height and four vegetation indices, including the normalized difference vegetation index (NDVI), green normalized difference vegetation index (GNDVI), enhanced vegetation index (EVI), and green chlorophyll index (GCI), for three mangrove plant species in the flying area. *Bruguiera gymnorrhiza* and *Rhizophora stylosa* reach an average height of 4 to 5 m and are distributed mainly in high tide areas. Meanwhile, *Kandelia obovata* has a lower height (ranging from 2 to 4 m), distributed in low-tide areas, near frequent flows. This study confirms the superiority of UAV with red edge and near-infrared wave bands in classifying and studying mangrove structures in small-scale areas.

KEYWORDS: Wetland; Tree height; Near infrared; Tree species classification; Biodiversity assessment

CITATION: Ngo D. T., Quoc K. N., Dang N. T., Dang C. H., Tran L. L. and Nguyen H. D. (2023). Analysis Of The Mangrove Structure In The Dong Rui Commune Based On Multispectral Unmanned Aerial Vehicle Image Data. Geography, Environment, Sustainability, 4(16), 14-25

https://DOI-10.24057/2071-9388-2023-2641

ACKNOWLEDGEMENTS: This work was performed with the support of the project «Application of remote sensing technology and unmanned aerial vehicle to assess the change of wetland ecosystems» chaired by the Institute of Tropical Ecology, Joint Vietnam-Russia Tropical Science and Technology Research Center.

Conflict of interests: The authors reported no potential conflict of interest.

INTRODUCTION

With an area of approximately 7-9 million km^2, accounting for approximately 4-6% of the land surface, wetlands play a very important role in human life, including approximately 45% of the natural value of ecosystems (Costanza et al. 1997; Mitsch et al. 2000). Despite the importance of flooding, approximately 50% of the world's wetlands have been lost since the 1900s (Nicholls 2004). In Vietnam, mangrove areas have also been significantly reduced, with approximately 4/5 of the total mangrove area disappearing between 1943 and 2003 (IUCN 2012). Therefore, classification and assessment of the structure and status of mangroves are considered the basis for developing management, monitoring and conservation measures (Pellegrini et al. 2009).

Mangroves are ecosystems with a diverse level of salt-tolerant species composition, mainly woody trees commonly found in intertidal, tropical and subtropical coastal areas (Polidoro et al. 2010). Mangroves play a huge role in preventing coastal erosion, mitigating wave impacts, and protecting coastal habitats (Nguyen, H. H. et al. 2020). In addition, mangroves have other important functions, such as breeding and nesting grounds, shelter areas, nurseries, and feeding habitats (Nagelkerken et al. 2008). For mangrove ecosystems, the distribution of species is different, mainly along the slopes of tidal flat terrain (Watson 1925). Based on the properties and

capabilities of mangroves, it is possible to classify different mangrove biomes, thereby providing an overview of the types of mangrove biomes and the dominant interactions that form them (Saenger 2002).

In the past, the method of dividing cells and establishing cross sections was commonly used to study mangrove structures such as species composition, tree density and tree height, trunk diameter, root density, and tree height (Dawes 1999; Ly et al. 2016). LiDAR technology has the ability to provide height and canopy structure parameters and is also widely used in forest plant taxonomy studies (Andersen et al. 2005; Brennan et al. 2006; Maltamo et al. 2004; Zhang 2020). In addition to field measurements, satellite images are effective tools for analysing and assessing the structure, function and area fluctuations of mangrove biomes (Nguyen, H. H. et al. 2020; Nguyen, L. D. et al. 2019). At Kecebing Bay, Sentinel-2 satellite imagery was applied to analyse the vertical and horizontal structure as well as the abundance of mangrove biomes (Nur W et al. 2017). However, satellite images are often low resolution, leading to errors in the results of structural analysis of mangroves.

To limit the errors caused by low image resolution, unmanned aerial vehicles (UAV) are considered an effective solution for providing ultrahigh-resolution images (Bandini et al. 2017; Lorenz et al. 2017). UAV are capable of providing resolutions of up to several centimetres, allowing them to determine the detailed structure of forest vegetation, such as measuring forest canopy gaps (Nguyen, D. H. et al. 2021), identifying vegetation index types (Mallmann et al. 2020; Ngo et al. 2020), creating tree classification maps (Hese et al. 2019), and constructing forest routes (Buğday 2018). With the improvement of cameras mounted on UAV, especially UAV with multispectral cameras, including near-infrared wave bands, many different types of vegetation indices can be identified (Hunt et al. 2013). Types of UAV with sensors, including red-edge and near-infrared (NIR) wave bands, for measuring vegetation indices have recently been introduced in agricultural research (Yeom et al. 2019). Vegetation indicators are important indicators in determining the health status of crops and types of vegetation (Modi et al. 2019). For UAV data, some types of vegetation indicators are commonly used in vegetation studies, such as the normalized difference vegetation index (NDVI) (Pal et al. 2020; Song et al. 2020), enhanced vegetation index (EVI), soil-adjusted vegetation index (SAVI) (Rhyma et al. 2019), and soil-atmospherically resistant vegetation index (SARVI) (Qiao et al. 2022).

In addition to the ability to provide various types of vegetation indicators for determining the health and structure of vegetation, the images obtained from UAV are also capable of classifying tree species and determining the height of dominant plant biomes (Deng et al. 2022; Huang et al. 2019; Okojie 2017). In the wetland area of Florida, UAV are applied in the classification of seven land use mantle objects using object-based image analysis (OBIA) (Liu et al. 2018). In the rich Central European forest area, UAV are used to classify plants based on the reflection spectrum of each plant species with an accuracy of 78.4% (Richter et al. 2016). In India, UAV are also used in the classification of detailed coating types with up to 95% accuracy (Richter et al. 2016; Tiwari et al. 2020). In Luozhuang, Changziying town, China, the authors used images obtained from UAV to classify eight mantle objects, including six different tree species (Yunjun et al. 2019). Tree height determination studies from the Digital Surface Model (DSM) after image processing UAV were also applied in various regions (Huang et al. 2019). In India, UAV were tested to determine the height of oil palm trees (Abdullah et al. 2022). In the Czech Republic, UAV are used to determine the height of *Picea abies L., Larix decidua, Pinus sylvestris,* and *Betula* lines ranging from 11.42 to 12.62 m (Panagiotidis et al. 2018).

In addition to being able to provide ultrahigh-resolution images, UAV also have significant advantages in studying the structure of mangrove vegetation. The images obtained from UAV are optimal methods for accurately mapping mangrove characteristics with canopy characteristics, biome types, and coverage (Kamal et al. 2014). UAV with multispectral sensors can provide and determine correlations between the NDVI vegetation index, canopy height, and canopy coverage (Yaney-Keller et al. 2019; Zahra et al. 2022). Combining the sensors available on UAV and LiDAR technology enables the detection and measurement of tree height and canopy diameter and the determination of cluster density (ma et al. 2017; Prasetyo et al. 2019; Yin et al. 2019). High-resolution imagery from UAV allows accurate identification of forest canopy gaps and assessment of their fluctuations over periods for mangrove ecosystems, thereby serving as a basis for monitoring the recovery of tree canopies (Lassalle et al. 2022). For wetland areas, the advantage of UAV is that they can be used to capture images actively at any time, right at local flooding or at low tide (Dezhi et al. 2018). However, the use of UAV in vegetation research also faces some limitations in adverse weather conditions, such as the effects of wind and rain conditions due to small loads (Matese et al. 2015; Nex et al. 2014).

Dong Rui commune mangroves are regarded as one of the two most diversified mangrove habitats in northern Vietnam that must be properly maintained (Huan 2021). However, past research has solely concentrated on measuring species composition, biodiversity levels, and area variations caused by aquaculture operations and local fishing. One of the key markers controlling the development of this ecosystem is the structure and distribution of mangrove plant species (Sarno et al. 2015). The use of UAV for the structural evaluation of mangrove ecosystems will provide a more comprehensive picture of the structure, variety, and species composition of wetland ecosystems in Dong Rui commune. In particular, this research has applied multispectral UAV for the first time in studying plant structure and classification in mangrove forests in Dong Rui commune. This result is the basis for the planning and conservation of mangrove plant biomes belonging to the wetland ecosystem for the Dong Rui commune area.

In this study, a Phantom 4 Multispectral UAV was used to photograph mangrove biomes outside the dike in the wetlands of Dong Rui commune, Tien Yen district, Quang Ninh province, Vietnam. Here, the distribution and structure of each plant biome from the dike to the outside of the estuary are markedly different. The main goal of the study is to determine the structure of mangrove biomes based on the following criteria: tree subspecies, tree height and several different vegetation indicators.

MATERIALS AND METHODS

Study area

The Dong Rui commune wetland area covers an area of 4902 hectares, with geographical coordinates from 21°11'N to 21°33'N and from 107°13'E to 107°32'E (Figure 1). This is a coastal accretion area with low terrain, gradually moving to the sea and an average elevation from 1.5 meters to 3 meters. Many places are renovated into arable land and aquaculture lagoons, and the rest are parrot beaches and

coastal dunes flooded with tidal water. The saline soil group dominates the research area, and the alluvial soil in the central area is where the local population is concentrated.

In estuary biomes, abundant mangroves appear in tidal wetlands, adapt to unstable conditions of the environment and are affected by low and high tides. Due to the terrain conditions of the narrow estuary marshes distributed along the riverbank, this type of carpet is a group of trees that grow scattered and take the form of strips. Characteristic plant biomes include Aegiceras corniculatum superior plant biomes with the plant associations of *Aegiceras corniculatum, Kandelia obovata, Bruguiera gymnorhiza, and Rhizophora stylosa, Aegiceras corniculatum, and Kandelia obovata,* and *Kandelia obovata, Bruguiera gymnorhiza, and Rhizophora stylosa.*

Flight procedures for capturing and processing UAV

This study used a DJI Phantom 4 Multispectral UAV with 6 cameras combined with RTK positioners that provide a multispectral imaging system consisting of 1 RGB camera and a multispectral camera array with 5 cameras covering the following bands: Blue (R_b): 450 nm ± 16 nm, Green (R_g): 560 nm ± 16 nm, Red (R_r): 650 nm ± 16 nm, Red edge (R_{re}): 730 nm ± 16 nm, and Near-infrared (R_{nir}): 840 nm ± 26 nm – all at 2 MP.

The UAV flight route was built with DJI GPS Pro software with the following flight parameters: UAV flight altitude: 60 m; photo coverage: 80%; flight time: 7h00 to 8h00 at the lowest tide; flight date: July 15, 2022.

After flying, UAV image data will be processed using Pix4Dmapper Enterprise 4.4.12 software according to the process in Fig. 3.

Tree-species classification

Tree-species classification

Based on field surveys, a set of image sequences were collected from mangrove tree taxonomic samples consisting of three species: *Bruguiera gymnorrhiza, Rhizophora stylosa,* and *Kandelia obovata.* Next, the image interpretation key is fed into the eCognition software that implements the multiresolution segmentation algorithm. Baatz (2000) developed and used the multiresolution

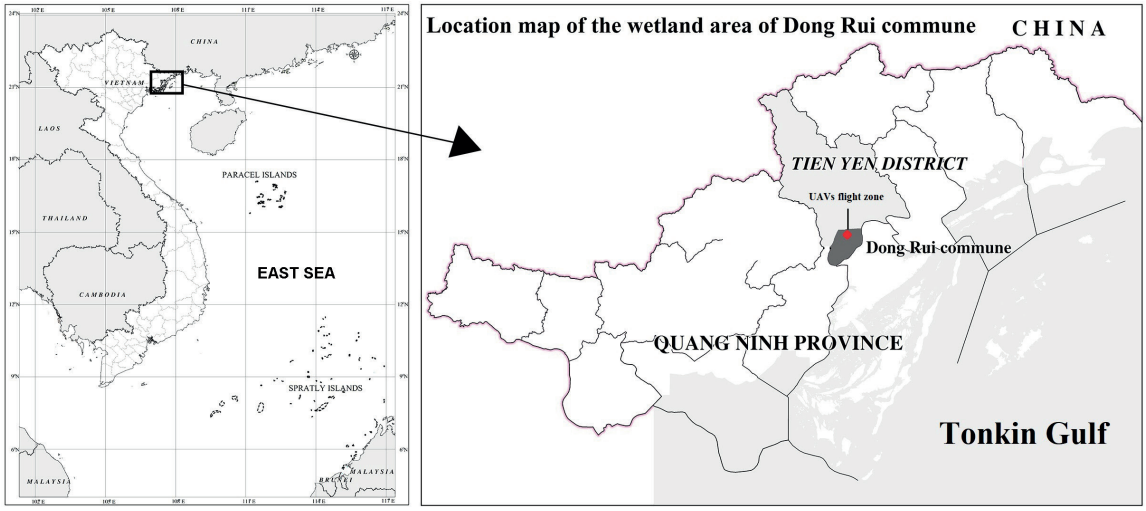

Fig. 1. Map of the location of the Dong Rui commune wetland area

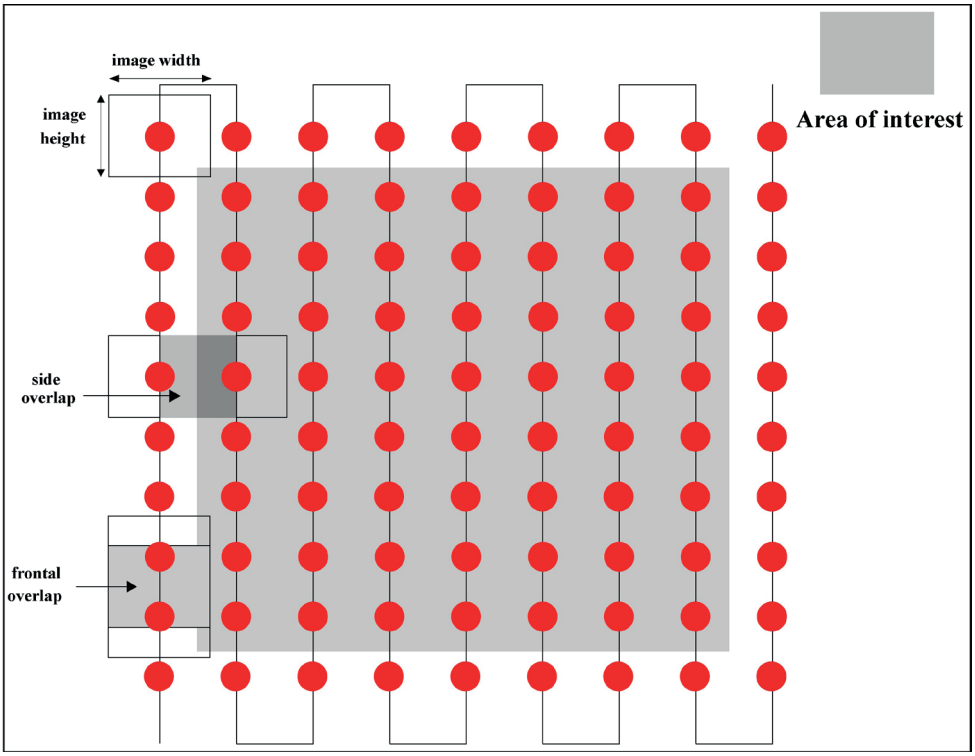

Fig. 2. Flight routes for UAV

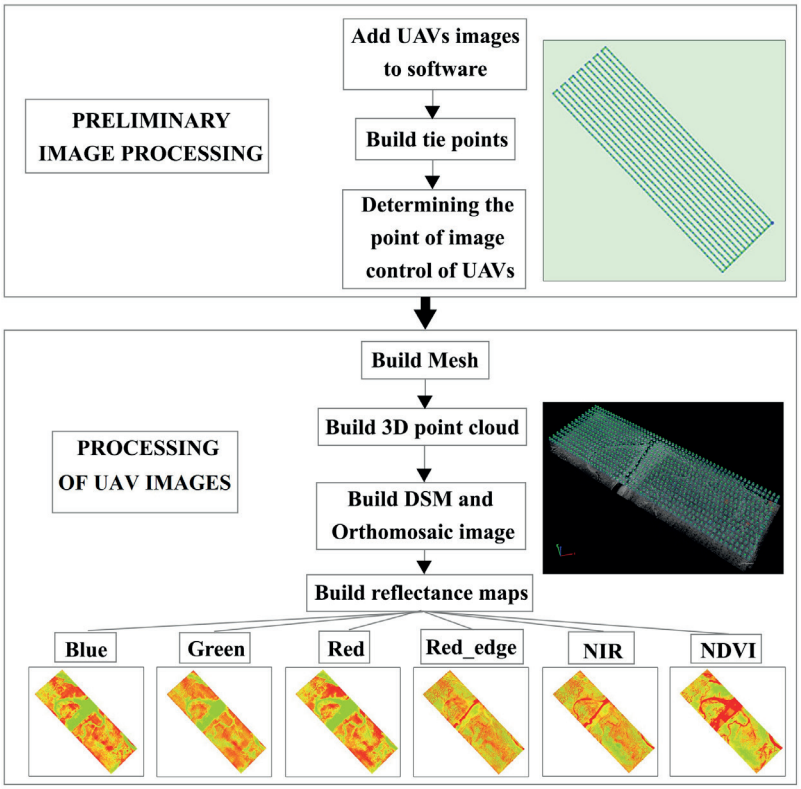

Fig. 3. UAV image processing process

segmentation algorithm, which is a fusion technique for grouping regions with similar pixels and adjacent points into objects by considering the homogeneity criteria of existing pixels or image objects (Baatz et al. 2000). Multiresolution segmentation algorithms are based on the principle of maximizing uniformity in objects and heterogeneity between objects (Chen et al. 2019). Photo segmentation is used to locate objects and boundaries between objects (Kavzoglu et al. 2014). In the next steps, smaller image objects are merged into larger objects.

To enhance the accuracy of mangrove vegetation classification maps in the Dong Rui commune, this study used the random forest algorithm. Random forests, proposed by Breiman, allow the classification of forest trees by the regression method (Breiman L. 2001). The random forest algorithm includes two additional pieces of information: a measure of the importance of the predictor variables and a measure of the internal structure of the data (the proximity of different data points to one another). Currently, the random forest algorithm is widely used in classification, forest inventory mapping, and forest tree classification, helping to enhance the accuracy of different types of thematic maps (Francke et al. 2008; Prinzie et al. 2007).

Map accuracy assessment

The error matrix (confusion matrix) between the classification results and the control sample was constructed, and the kappa coefficient (K) was evaluated. Kappa was first introduced in 1960 by Cohen as a reliability statistic when two judges classified targets into categories on a nominal variable (Cohen, 1960). The Kappa coefficient is a suitable tool for assessing the reliability of maps based on preliminary results and factual verification results and is used in many studies of remote sensing-based mapping (Nguyen, D. H. et al. 2022; Pardo-Iguzquiza et al. 2018).

Accordingly, 20% of the total number of photo reference samples collected in the field (corresponding to 558 photo reference samples) was used to assess map accuracy (Fig. 4). The kappa coefficient was used as a measure of classification accuracy. This is the utility factor of all the primes from the error matrix. It is the essential distinction between what is true about the matrix's deviation error and the total number of changes reflected by the rows and columns. The formula for determining the kappa index is as follows:

$$K = \frac{N\sum_{i=1}^{r} X_{ii} - \sum_{i=1}^{r}\left(X_{i+} - X_{+i}\right)}{N^2 - \sum_{i=1}^{r}\left(X_{i+} - X_{+i}\right)} \quad (1)$$

Here, r is the number of columns in the image matrix, X_{ii} is the number of pixels observed in row i and column i (on the main diagonal), X_{i+} is the total pixels observed in row i, and N is the total number of pixels observed in the image matrix.

The kappa coefficient is usually between 0 and 1; values in this range indicate acceptable accuracy of the classification. Kappa can be classified into three groups of values: $K \geq 0.8$: high accuracy; $0.4 \leq K < 0.8$: moderate accuracy; and $K < 0.4$: low accuracy (US Geological Survey).

Determination of mangrove vegetation structure based on UAV

Determination of tree height

To determine the height of the mangrove biome in the study area, a terrain number model (DTM) and surface number model (DSM) (Fig. 5) were constructed from point cloud data from images obtained by UAV (Al-Najjar et al. 2019). To improve the accuracy of the DTM model, in addition to the GPS measurement data in the field, this study identified ground points directly based on forest canopy gaps obtained from UAV images. The tree height in the study area is calculated by subtracting the DSM value from the DTM value (Lisein et al. 2013).

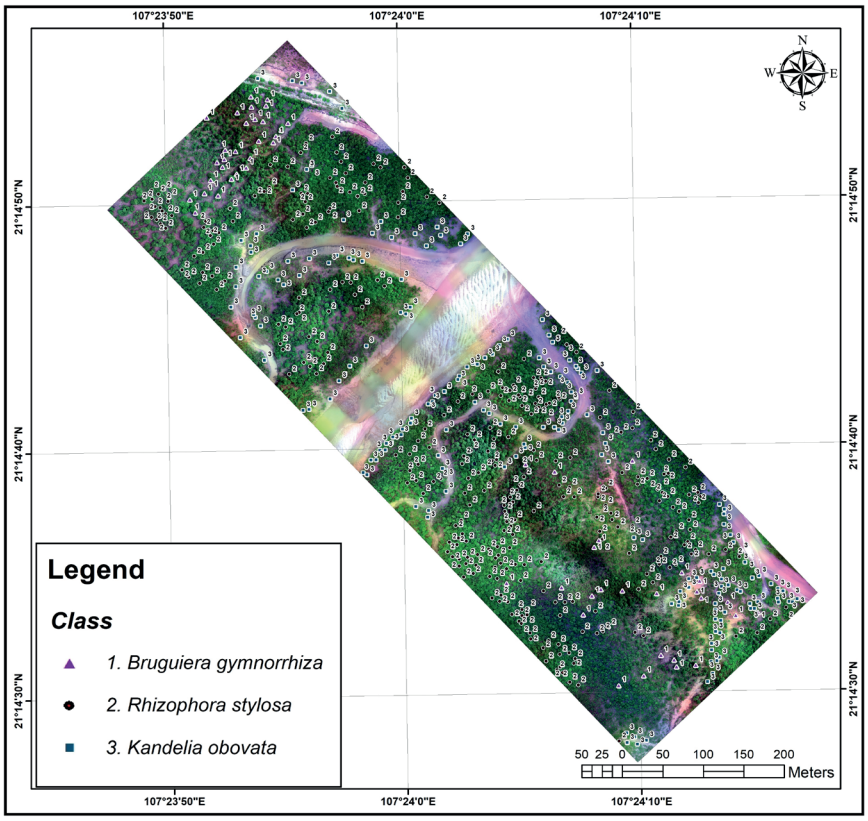

Fig. 4. 558-point image lock diagram for map accuracy assessment

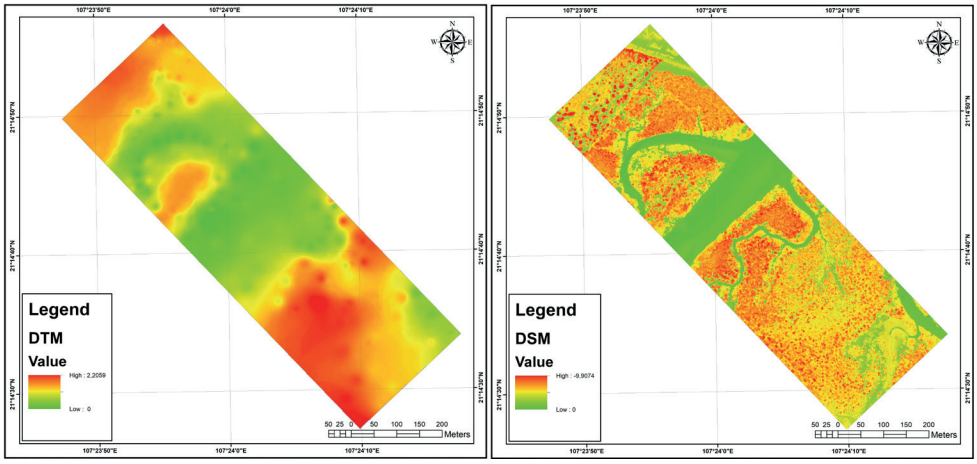

Fig. 5. Model DTM and DSM flight area capture UAV

Identification of vegetation indices

Based on 5 monochrome spectral channels obtained after UAV image processing (blue (R_b): 450 nm ± 16 nm, green (R_g): 560 nm ± 16 nm, red (R_r): 650 nm ± 16 nm, red edge (R_{re}): 730 nm ± 16 nm, near-infrared (R_{nir}): 840 nm ± 26 nm)), several vegetation indices for mangrove areas were identified, including the following:

Normalized Difference Vegetation Index (NDVI). This is an important indicator in studies of ecology, growth, development and fluctuations in plant cover. In addition, this indicator also contributes to warnings about crop disease status, yield and crop yields when combined with other indicators. The NDVI index has many applications in agriculture and forestry. In particular, applications to detect plant cover fluctuations between different periods on one fixed range. In addition, in the field of agriculture, the NDVI index also contributes to the assessment of crop development and the forecast of yield. The NDVI index is calculated by the formula (Tucker, 1979):

$$NDVI = \frac{R_{nir} - R_r}{R_{nir} + R_r} \quad (2)$$

Green Normalized Difference Vegetation Index (GNDVI). Similar to the NDVI, the GNDVI further enhances the variability in chlorophyll in plant leaves. The GNDVI is calculated by the following formula (Hunt et al. 2013):

$$GNDVI = \frac{R_{nir} - R_g}{R_{nir} + R_g} \quad (3)$$

The enhanced vegetation index (EVI) was invented by Liu and Huete to simultaneously calibrate the value of NDVI against atmospheric influence and ground reflection, particularly in areas with dense canopies. The value range of the EVI is -1 to 1; for healthy vegetation, the EVI value ranges between 0.2 and 0.8. The formula for calculating the EVI index is as follows (Huete et al. 2002):

$$EVI = 2.5 \frac{R_{nir} - R_r}{R_{nir} + 6R_r - 7.5R_b + 0.16} \quad (4)$$

Green Chlorophyll Index (GCI). In remote sensing, the green chlorophyll index is used to estimate the chlorophyll content in various plant species. The chlorophyll content reflects the

physiological state of vegetation; it decreases in stressed plants and thus can be used as a measurement of plant health. The GCI index is calculated by the formula (Hunt et al. 2013):

$$GCI = \frac{R_{nir}}{R_g} - 1 \quad (5)$$

RESULTS

Mangrove tree-species classification map

Map accuracy assessment

Based on the 558 reference samples used to assess the map accuracy and classification results of each mangrove plant species at the UAV flying area, a matrix table was developed to assess the accuracy of the mangrove species classification map (Tab. 1).

Accordingly, the overall accuracy of the UAV classification map is 86.28%, corresponding to K=0.84 (according to formula 1). Compared to the K range given by the US Geological Survey, what is the high accuracy (K ≥ 0.8).

For user accuracy, *Kandelia obavata* had the highest value, reaching 98.06%, and the lowest belonged to the species *Bruguiera gymnorrhiza*, with a value of only 71.88%. For producer accuracy, the highest value belonged to *Rhizophora stylosa*, which scored 93.69%, while *Kandelia obovata* had the lowest value, reaching 81.28% (Tab. 1). According to Table 1, only 14% of the total number of samples (corresponding to 8/54 samples) of *Bruguiera gymnorrhiza* were misinterpreted as *Rhizophora stylosa*. Meanwhile, 5.36% of all specimens of *Rhizophora stylosa* were misinterpreted as *Bruguiera gymnorrhiza*, accounting for 17/317. For samples of the species *Kandelia obovata*, 18.13% of the total samples were misinterpreted as *Rhizophora stylosa*, corresponding to 34 of the 187 total samples of the species *Kandelia obovata* identified in the field.

Tree-species classification map

Based on the process of mapping mangrove vegetation taxonomy, taxonomic mapping was established, and the distribution was determined for 3 mangrove plant species, including *Bruguiera gymnorrhiza, Rhizophora stylosa*, and *Kandelia obovata*, in the UAV flight area (Fig. 6).

Table 1. Error matrix evaluates map accuracy

		Ground Reference			Total
		Bruguiera gymnorrhiza	*Rhizophora stylosa*	*Kandelia obavata*	
Classification	Bruguiera gymnorrhiza	**46**	8		**54**
	Rhizophora stylosa	17	**297**	3	**317**
	Kandelia obavata	1	34	**152**	**187**
Total		64	339	155	**558**
User Accuracy (%)		71.88	87.61	98.06	**85.85**
Producer Accuracy (%)		85.19	93.69	81.28	**86.72**
Overall Accuracy (%)					86.28

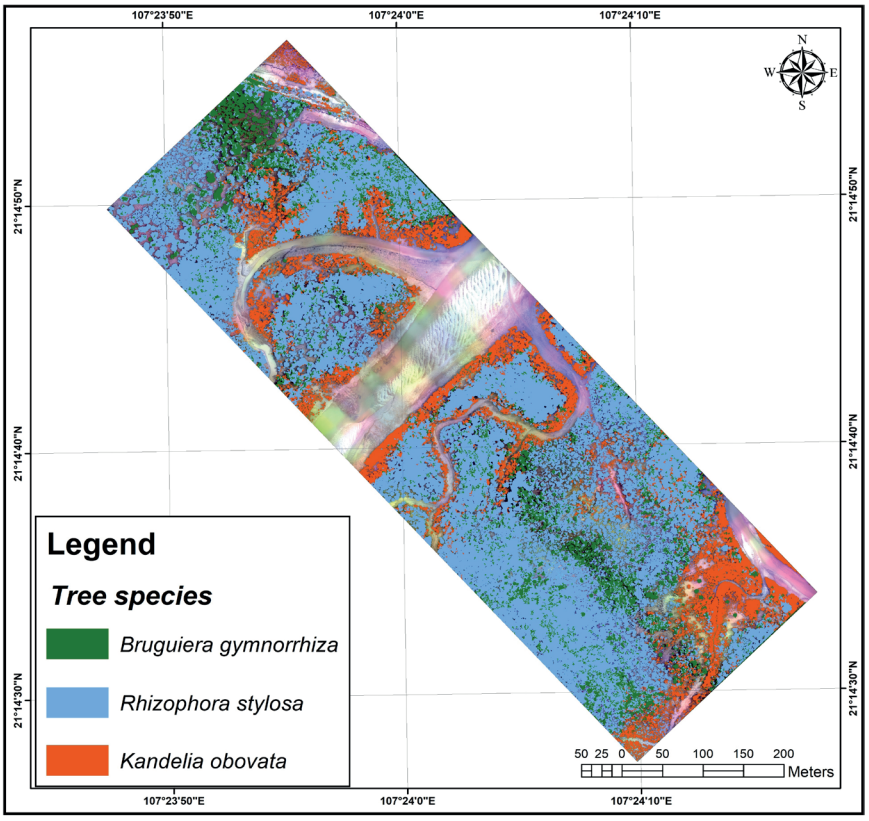

Fig. 6. Tree-species classification map of flying areas capturing UAV

In the study area, *Rhizophora stylosa* predominates, often with an alternating distribution with *Bruguiera gymnorrhiza* at high tide flats, creating vegetation populations that characterize not only UAV but also the western area of Dong Rui commune (Fig. 6). Meanwhile, *Kendelia obovata* is distributed mainly in low tide areas, riverine areas and areas along frequent streams (Fig. 6).

According to Fig. 7, the canopy coverage rate of *Rhizophora stylosa* is the highest of the 3 species identified in the UAV flight area, reaching 65.89% of the total area covered. Next, the coverage areas of *Bruguiera gymnorrhiza* and *Kendelia obovata* species were relatively low compared to *Rhizophora stylosa*, at 14.44% and 19.67%, respectively.

Mangrove structure

Tree height

Based on the established DSM and DTM models using UAV flight imagery data, a tree height map for the study area was developed (Fig. 8).

According to Fig. 8 and Tab. 2, the *Bruguiera gymnorrhiza* population has the largest height in the study area, particularly in the northern and central areas of the UAV (average height ranges from 4.41 ± 0.51 m). For *Rhizophora stylosa*, the height of some individuals in the northern region is also relatively large, and the average height reaches approximately 4.28 ± 0.68 m. The biome of *Bruguiera gymnorrhiza* and *Rhizophora stylosa* reaching an average height of 2 m to 4 m is concentrated mainly in the south and southeast of the UAV flying area, occupying most of the area.

Meanwhile, *Kendelia obovata* populations are distributed in low-tide areas at lower elevations than those of *Bruguiera gymnorrhiza* and *Rhizophora stylosa*, averaging only 3.47 ± 0.63 m. Some of the *Kendelia obovata* bodies located in the north and south of the flight area capture UAV with a height of only approximately 1.5 m (Fig. 8).

According to Figs. 6 - 8, the strong growth of *Bruguiera gymnorrhiza* and *Rhizophora stylosa* biomes can be seen in the UAV, with a predominance in both area distribution and tree height. Meanwhile, *Kendelia obovata* predominates in low-tide, riparian or frequent streams.

Vegetation indices of mangroves

According to the formula for calculating vegetation indices (Formulas 2-5), four maps have been developed showing the value of vegetation indices for UAV, including NDVI (Fig. 9a), GNDVI (Fig. 9b), EVI (Fig. 9c), and GCI (Fig. 9d).

According to Fig. 9a, areas with the distribution of *Bruguiera gymnorrhiza* and *Rhizophora stylosa* species have higher NDVI values than areas with only the distribution of

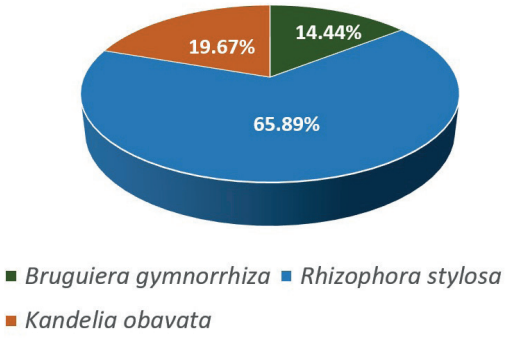

Fig. 7. The canopy coverage ratio of 3 types of flying area plants captured by the UAV

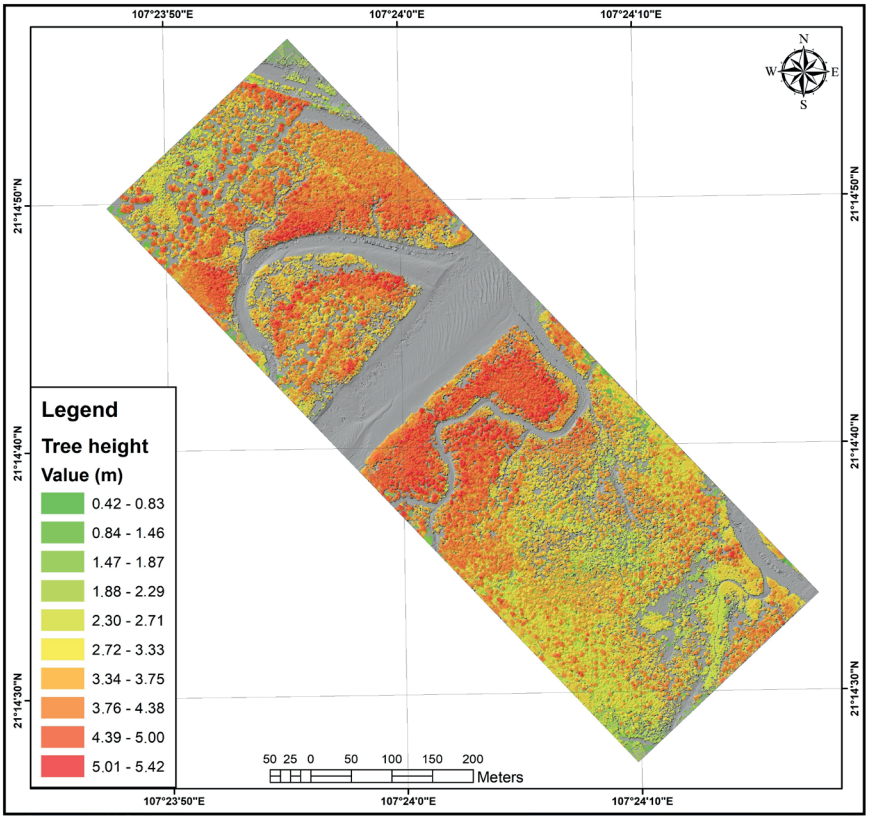

Fig. 8. Tree height map of flying area capturing UAV

Table 2. Number of individuals, mean ± standard deviation, minimum and maximum tree height

Species	Number of individuals	Mean height ± S.D. (m)	Min. - Max. Height (m)
Bruguiera gymnorrhiza	54	4.41 ± 0.51	3.54 – 5.42
Rhizophora stylosa	317	4.28 ± 0.68	1.25 – 5.42
Kendelia obovata	187	3.47 ± 0.63	1.46 – 5.21

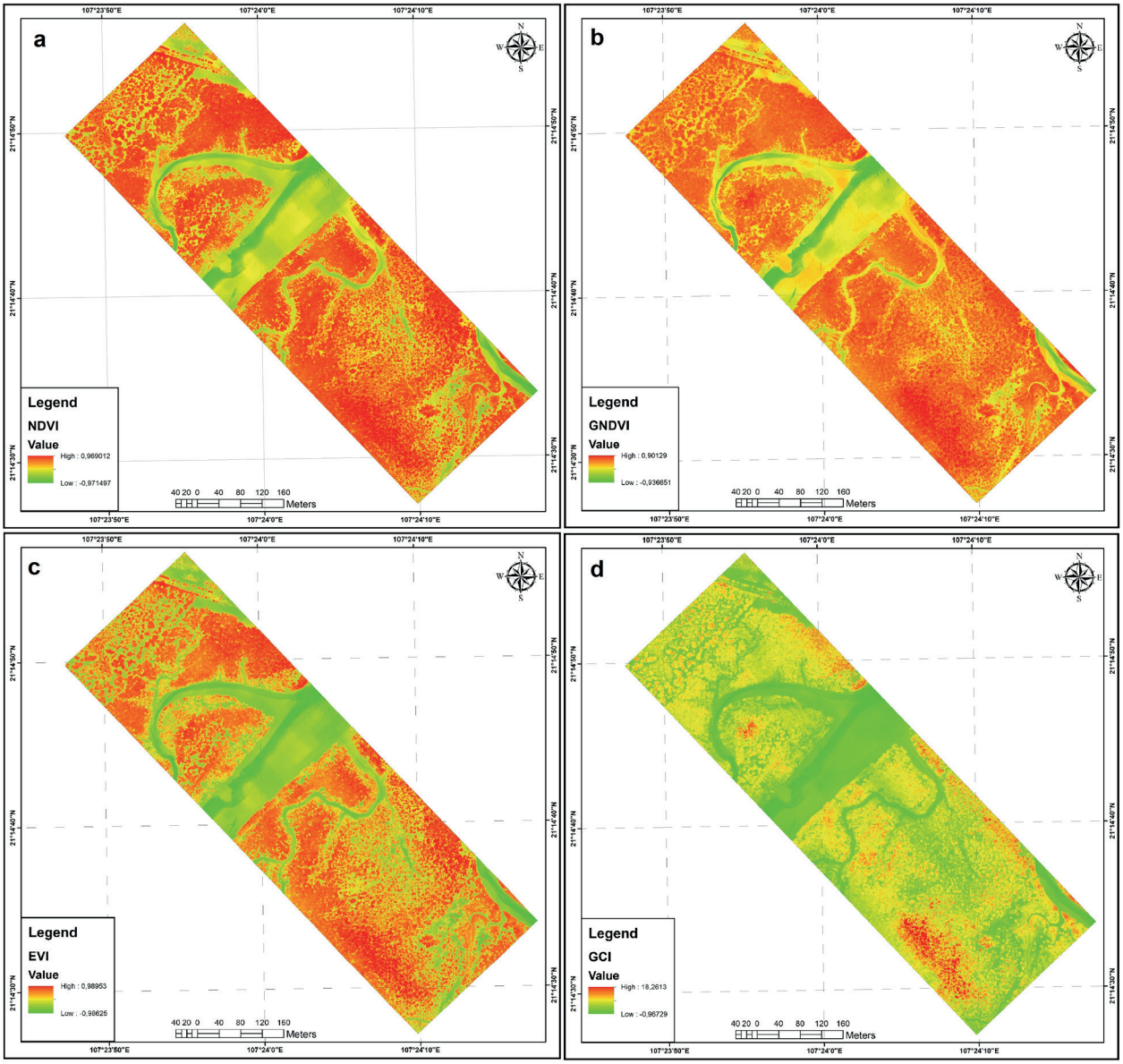

Fig. 9. Values of some vegetation indices in the UAV flying area

Kendelia obovata species. In particular, areas with high NDVI values in the mangrove biome area have a large height (ranging from 4 m to 5 m) and large coverage. Similar to the NDVI value, the high GNDVI and EVI values in this area are also concentrated in the *Bruguiera gymnorrhiza* and Rhizophora stylosa biomes, which have reached a stable state, high height, and high coverage (Fig. 9b, 9c). For the GCI value, the flora consists of *Bruguiera gymnorrhiza* and *Rhizophora stylosa* species distributed in the south and northeast of the most valuable UAV flight area (Fig. 9d).

Based on 558 field sampling points, 4 types of vegetation index values (NDVI, GNDVI, EVI, and GCI) were extracted from each point to compare the values of vegetation index types between mangrove species. According to Fig. 10, the NDVI and EVI values of *Bruguiera gymnorrhiza* and *Rhizophora stylosa* are similar, achieving mean values of 0.82 and 0.76, respectively, higher than those of *Kendelia obovata* (average NDVI value reaches 0.68, EVI reaches 0.62). The EVI of vegetation at all sampling sites was greater than 0.2, indicating that the state of mangrove health at the UAV was good. For the GNDVI value, the value of the above three species is relatively large, reaching between 0.62 and 0.68, of which the highest is the species *Bruguiera gymnorrhiza* (Fig. 10). The GCI values of these three plants varied widely, with the mean GCI values of *Bruguiera gymnorrhiza, Rhizophora stylosa*, and *Kendelia obovata* being 4.4, 3.7, and 3.2, respectively (Fig. 10).

DISCUSSION

This study provides a method for classifying mangrove trees based on data obtained from UAV and analyses the mangrove structure in the Dong Rui commune based on height parameters and vegetation indicators determined by the results of multispectral UAV. This is the advantage of photos taken because UAV have a multispectral camera with

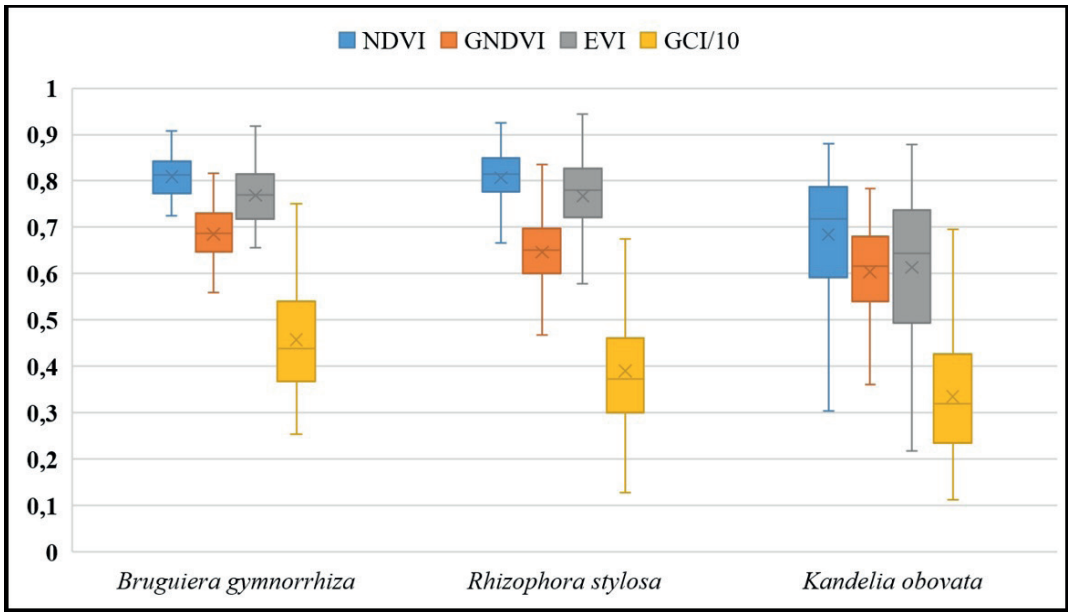

Fig. 10. Value of vegetation indices of three species of mangrove trees flying area shooting UAV

5 monochrome wave bands (green, blue, red, red_edge, and NiR), allowing up to 21 different vegetation indicators to be identified (Hunt et al. 2013), while conventional UAV only mount cameras with RGB wavebands that only allow the identification of some vegetation indicators, such as VARI and TGI (Ngo et al. 2020). Analysis of vegetation indicators is considered an effective method in the classification and assessment of mangrove vegetation texture (Cao et al. 2018).

Combining imaging and random forest algorithms with the characteristic spectra of each plant allows for enhanced accuracy of mangrove classification maps (Jiang et al. 2021). In the UAV flight area, 3 species of trees, including *Bruguiera gymnorrhiza, Rhizophora stylosa,* and *Kendelia obovata,* were classified with an overall accuracy of 86.28%, corresponding to K=0.84. These are 3 species of mangrove plants common in the tidal flat area of the Dong Rui commune. Almost all mangrove species are distinguishable in the visible and near-infrared infrared because of the dispersion in porous mesenchymal cells in plants (Zulfa et al. 2021; Zulfa et al. 2020). In addition to the image classification method combined with random forest terminology, the determination of chlorophyll content in plant leaves according to plant indicators based on spectroscopic measurements is also a common method for classifying plants (Meivel et al. 2023; Xue et al. 2009). Botanical indicators using a wave range from 550 nm to 730 nm are suitable for plant classification purposes due to the different leaf structures of each species (Zhao et al. 2019). The wavelengths of 549 nm, 559 nm, 702 nm, 722 nm, 742 nm, and 763 nm are the most sensitive to the chlorophyll of mangrove tree species (George et al. 2020).

The average NDVI value of mangrove vegetation in Dong Rui commune in both summer and winter ranges from 0.7 to 0.8, which is higher than the average NDVI value of mangrove forest areas in Dodola and Guraping of North Maluku Province (Singgalen 2022) or North Halmahera, Indonesia (Singgalen et al. 2021) when the average NDVI value in these areas is only 0.3 to 0.4. The NDVI value of mangroves in the Dong Rui commune is greater when compared to the NDVI value of the Can Gio mangrove forest region, a typical mangrove forest area in southern Vietnam (Hoa et al. 2020). Dong Rui commune mangroves have NDVI and GNDVI values that are comparable to those found on Sumatra's eastern coast (NDVI = 0.738 and GNDVI = 0.641) (Samsuri et al. 2021) and greater than those found in the Banten, Jakarta, and West Java Ecotone Zones (NDVI: 0.39 – 0.61 and GNDVI: 0.25 – 0.48) (Asy'Ari et al. 2022).

According to the results of the biodiversity survey of the research team in the wetland area of the Dong Rui commune, the level of species diversity here is relatively large when compared to other wetland areas in northern Vietnam, such as the Cat Ba mangrove forest, Phu Long – Gia Luan mangrove forest, and Hai Phong Province (Pham et al. 2017; Thinh et al. 2008). In Xuan Thuy National Park (Nam Dinh Province), the wetland ecosystem is considered the most diverse in northern Vietnam, and the biodiversity level of the species composition of the Dong Rui commune wetland area is equivalent to over 1500 species of organisms (Huan 2021; Nhan et al. 2015).

In the wetland area of the Dong Rui commune, the height of mangrove plant biomes is relatively low. For the biomes of *Bruguiera gymnorrhiza, Rhizophora stylosa* tidal flats, their average height is only 4 – 5.5 m. Compared with the mangrove areas of southern Vietnam, such as U Minh Ha National Park (*Melaleuca alternifolia* height can be up to 10-12 m) (Safford et al. 1998) or Tram Chim National Park (Viet et al. 2020), this is a much lower tree height. There are many reasons for the difference in the structure of mangrove flora between southern and northern Vietnam, mainly because the sediment layer of mud and sand in the northern region is thinner than that in the southern area (Huan 2021). In addition, northern Vietnam is subject to many impacts from typhoons (average 5.2 typhoons/year) (Toan, 2014). Therefore, the mangrove plant biomes here cannot reach great heights (People's Committee of Tien Yen district 2015; Van et al. 2022). Similarly, when compared to some mangrove areas in Southeast Asia, such as in Perak Province, Malaysia (Otero et al. 2018), Indonesia (FAO 2007) or in the world, such as in the Czech Republic (Panagiotidis et al. 2018), the average height of mangroves in Dong Rui commune is much smaller.

The classification of plants based on UAV imagery is still mainly based on spectral values and canopy morphology on the resulting images, which do not show other morphological forms, such as stem and root structures. These are the limitations of classifying plants based on UAV data, which do not represent tree structures below the foliage, which are already obscured by the canopy. To limit errors when classifying mangrove trees based on satellite imagery, verifiable field surveys are indispensable. In addition, lidar sensors are also suitable tools for analysing mangrove structures (Doughty et al. 2021).

CONCLUSIONS

In this study, based on multispectral UAV image data, tree classification maps and mangrove structure analysis through tree height values and vegetation index values were developed for UAV flight zones in the Dong Rui commune wetland ecosystem. Combined with collecting tree taxonomy samples through field surveys and image processing methods of UAV on GIS software, we propose that UAV are effective tools for small-scale mangrove structure classification and assessment.

However, the limitation of UAV is that the range of operations is limited to only approximately 200 hectares. Therefore, mapping large-scale areas is more efficient when combined with high-resolution satellite imagery along with UAV that are "key points" to identify details for small areas. In addition, the enhanced combination with lidar sensors will help to establish a more detailed model of the structure of vegetation.

Based on the findings of this research, local managers may create programs and strategies to examine the present state of the structure, number, and function of each species participating in the Dong Rui commune mangrove ecosystem. Furthermore, the findings of this research may be used to measure the amount of growth of each species in various intertidal locations, which can then be utilized to pick restored mangrove seedlings for each appropriate site. UAVs are also useful for assessing and monitoring topography alterations as well as the sedimentation of estuary sediments based on seasonal or yearly cycles. With the development of UAV technology in the future, such as enhanced image resolution, resistance to extreme weather conditions or increased flight time, UAV will be a powerful support tool for researchers as well as managers in managing and conserving wetland ecosystems.

REFERENCES

Abdullah, S., Tahar, K. N., Abdul Rashid, M. F., & Osoman, M. (2022). ESTIMATING TREE HEIGHT BASED ON TREE CROWN FROM UAV IMAGERY. Malaysian Journal of Sustainable Environment, 9, 99. doi: 10.24191/myse.v9i1.17294

Al-Najjar, H., Kalantar, B., Pradhan, B., Saeidi, V., Abdul Halin, A., Ueda, N., & Mansor, S. (2019). remote sensing Land Cover Classification from fused DSM and UAV Images Using Convolutional Neural Networks. Remote Sensing, 2019, 1461. doi: 10.3390/rs11121461

Andersen, H.-E., McGaughey, R., & Reutebuch, S. (2005). Estimating forest canopy fuel parameters using LIDAR data. Remote Sensing of Environment, 94, 441-449. doi: https://doi.org/10.1016/j.rse.2004.10.013

Asy'Ari, R., Rahmawati, A., Sa'diyya, N., Gustawan, A., Setiawan, Y., Zamani, N., & Pramulya, R. (2022). Mapping mangrove forest distribution on Banten, Jakarta, and West Java Ecotone Zone from Sentinel-2-derived indices using cloud computing based Random Forest. Jurnal Pengelolaan Sumberdaya Alam dan Lingkungan (Journal of Natural Resources and Environmental Management), 12, 97-111. doi: https://doi.org/10.29244/jpsl.12.1.97-111

Baatz, M., & Schape, A. (2000). Multiresolution segmentation: an optimization approach for high quality multi-scale image segmentation. Angew. Geogr. Info. verarbeitung, Wichmann-Verlag, Heidelberg, 12-23.

Bandini, F., Butts, M., Jacobsen, T., & Bauer-Gottwein, P. (2017). Water level observations from Unmanned Aerial Vehicles for improving estimates of surface water-groundwater interaction. Hydrological Processes, 31. doi: https://doi.org/10.1002/hyp.11366

Breiman L. (2001). Random forests. Machine Learning, 1(45), 5–32.

Brennan, R., & Webster, T. (2006). Object-oriented land cover classification of LIDAR-derived surfaces. Canadian Journal of Remote Sensing, 32. doi: https://doi.org/10.5589/m06-015

Buğday, E. (2018). Capabilities of using UAVs in Forest Road Construction Activities. 4, 56-62. doi: https://doi.org/10.33904/ejfe.499784

Cao, J., Leng, W., Liu, K., Liu, L., he, Z., & Zhu, Y. (2018). Object-Based Mangrove Species Classification Using Unmanned Aerial Vehicle Hyperspectral Images and Digital Surface Models. Remote Sensing, 10, 89. doi: https://doi.org/10.3390/rs10010089

Chen, Y., Chen, Q., & Jing, C. (2019). Multi-resolution segmentation parameters optimization and evaluation for VHR remote sensing image based on mean NSQI and discrepancy measure. Journal of Spatial Science, 66, 1-26. doi: 10.1080/14498596.2019.1615011

Cohen, J. (1960). A Coefficient of Agreement for Nominal Scales. Educational and Psychological Measurement, 20, 37-46. doi: https://doi.org/10.1177/001316446002000104?journalCode=epma

Costanza, R., Arge, Groot, R., Farberk, S., Grasso, M., Hannon, B., . . . Belt, M. (1997). The Value of the World's Ecosystem Services and Natural Capital. Nature, 387, 253-260. doi: https://doi.org/10.1016/S0921-8009(98)00020-2

Dawes, C. (1999). Mangrove structure, litter and macroalgal productivity in a northern-most forest of Florida. Mangroves and Salt Marshes, 3, 259-267. doi: 10.1023/A:1009976025000

Deng, T., Fu, B., Liu, M., He, H., Donglin, F., Li, L., . . . Gao, E. (2022). Comparison of multi-class and fusion of multiple single-class SegNet model for mapping karst wetland vegetation using UAV images. Scientific Reports, 12. doi: 10.1038/s41598-022-17620-2

Dezhi, W., Wan, B., Qiu, P., Su, Y., Guo, Q., Wang, R., . . . Wu, X. (2018). Evaluating the Performance of Sentinel-2, Landsat 8 and Pléiades-1 in Mapping Mangrove Extent and Species. Remote Sensing, 10, 1468. doi: https://doi.org/10.3390/rs10091468

Doughty, C. L., Ambrose, R. F., Okin, G. S., & Cavanaugh, K. C. (2021). Characterizing spatial variability in coastal wetland biomass across multiple scales using UAV and satellite imagery. Remote Sensing in Ecology and Conservation, 7(3), 411-429. doi: https://doi.org/10.1002/rse2.198

FAO. (2007). The world's mangroves 1980-2005 Food and Agriculture Organization of the United Nations. Rome.

Francke, T., López-Tarazón, J. A., & Schröder, B. (2008). Estimation of suspended sediment concentration and yield using linear models, Random Forests and Quantile Regression Forests. Hydrological Processes, 22, 4892-4904. doi: https://doi.org/10.1002/hyp.7110

George, R., Padalia, H., Kumar, S., & Sinha, S. (2020). Evaluating sensitivity of hyperspectral indices for estimating mangrove chlorophyll in Middle Andaman Island, India. Environmental Monitoring and Assessment, 191. doi: 10.1007/s10661-019-7679-6

Hese, S., Thiel, C., & Henkel, A. (2019). UAV based Multi Seasonal Deciduous Tree Species Analysis in the Hainich National Park using Multi Temporal and Point Cloud Curvature Features. Int. Arch. Photogramm. Remote Sens. Spatial Inf. Sci., XLII-2/W13, 363–370. doi: https://doi.org/10.5194/isprs-archives-XLII-2-W13-363-2019

Hoa, L., Tran, T., Gyeltshen, S., Nguyen, C., Tran, D., Luu, T., & Mán, D. (2020). Characterizing Spatiotemporal Patterns of Mangrove Forests in Can Gio Biosphere Reserve Using Sentinel-2 Imagery. Applied Sciences, 10, 4058. doi: https://doi.org/10.3390/app10124058

Huan, N. C. (2021). Established Dong Rui Wetland Reserve, Tien Yen, Quang Ninh Province (pp. 348). Quang Ninh: Department of Natural Resources and Environment of Quang Ninh province.

Huang, H., He, S., & Chen, C. (2019). Leaf Abundance Affects Tree Height Estimation Derived from UAV Images. Forests, 10, 931. doi: 10.3390/f10100931

Huete, A., Didan, K., Miura, T., Rodriguez, E., Gao, X., & Ferreira, L. G. (2002). Overview of the Radiometric and Biophysical Performance of the MODIS Vegetation Indices. Remote Sensing of Environment, 83, 195-213. doi: https://doi.org/10.1016/S0034-4257(02)00096-2

Hunt, J. E., Doraiswamy, P., McMurtrey, J., Daughtry, C., Perry, E., & Akhmedov, B. (2013). A visible band index for remote sensing leaf Chlorophyll content at the Canopy Scale. International Journal of Applied Earth Observation and Geoinformation, 21, 103–112. doi: https://doi.org/10.1016/j.jag.2012.07.020

Jiang, Y., Zhang, L., Yan, M., Qi, J., Fu, T., Fan, S., & Chen, B. (2021). High-Resolution Mangrove Forests Classification with Machine Learning Using Worldview and UAV Hyperspectral Data. Remote Sensing, 13, 1529. doi: https://doi.org/10.3390/rs13081529

Kamal, M., Phinn, S., & Johansen, K. (2014). Characterizing the Spatial Structure of Mangrove Features for Optimizing Image-Based Mangrove Mapping. Remote Sensing, 6, 984-1006. doi: 10.3390/rs6020984

Kavzoglu, T., & Yildiz, M. (2014). Parameter-Based Performance Analysis of Object-Based Image Analysis Using Aerial and Quikbird-2 Images. Paper presented at the Remote Sensing and Spatial Information Sciences, Gottingen.

Lassalle, G., & Souza Filho, C. (2022). Tracking canopy gaps in mangroves remotely using deep learning. Remote Sensing in Ecology and Conservation. doi: 10.1002/rse2.289

Lisein, J., Deseilligny, M., Bonnet, S., & Lejeune, P. (2013). A Photogrammetric Workflow for the Creation of a Forest Canopy Height Model from Small Unmanned Aerial System Imagery. Forests, 4, 922-944. doi: 10.3390/f4040922

Liu, T., & Abd-Elrahman, A. (2018). Multi-view object-based classification of wetland land covers using unmanned aircraft system images. Remote Sensing of Environment, 216. doi: https://doi.org/10.1016/j.rse.2018.06.043

Lorenz, S., Zimmermann, R., & Gloaguen, R. (2017). The Need for Accurate Geometric and Radiometric Corrections of Drone-Borne Hyperspectral Data for Mineral Exploration: MEPHySTo—A Toolbox for Pre-Processing Drone-Borne Hyperspectral Data. Remote Sensing, 9. doi: https://doi.org/10.3390/rs9010088

Ly, T. N., Van, P. D. T., Le, T. L., Jun, S., & Hisamichi, N. (2016). Mangrove structure variation under influences of tidal-inundation in the Bac Lieu coastal zone. Journal of Science and Technology.

ma, Q., Su, Y., & Guo, Q. (2017). Comparison of Canopy Cover Estimations From Airborne LiDAR, Aerial Imagery, and Satellite Imagery. IEEE Journal of Selected Topics in Applied Earth Observations and Remote Sensing, PP, 1-12. doi: 10.1109/JSTARS.2017.2711482

Mallmann, C. L., Zaninni, A. F., & Filho, W. P. (2020). Vegetation Index Based In Unmanned Aerial Vehicle (Uav) To Improve The Management Of Invasive Plants In Protected Areas, Southern Brazil. 2020 IEEE Latin American GRSS & ISPRS Remote Sensing Conference (LAGIRS), 66-69.

Maltamo, M., Eerikäinen, K., Pitkänen, J., Hyyppä, J., & Vehmas, M. (2004). Estimation of timber volume and stem density based on scanning laser altimetry and expected tree size distribution functions. Remote Sensing of Environment, 90, 319-330. doi: https://doi.org/10.1016/j.rse.2004.01.006

Matese, A., Toscano, P., Di Gennaro, S., Genesio, L., Vaccari, F., Primicerio, J., . . . Gioli, B. (2015). Intercomparison of UAV, Aircraft and Satellite Remote Sensing Platforms for Precision Viticulture. Remote Sensing, 7, 2971-2990. doi: https://doi.org/10.3390/rs70302971

Meivel, s., & Banu, D. (2023). Design and Method of an Agricultural Drone System Using Biomass Vegetation Indices and Multispectral Images (pp. 343-373).

Mitsch, W., & Gosselink, J. (2000). The Value of Wetlands: Importance of Scale and Landscape Setting. Ecological Economics, 35, 25-33. doi: https://doi.org/10.1016/S0921-8009(00)00165-8

Modi, A., & Das, P. (2019). Multispectral Imaging Camera Sensing to Evaluate Vegetation Index from UAV. Research & Reviews: Journal of Space Science & Technology, 8(2), 30-42.

Nagelkerken, I., Blaber, S. J. M., Bouillon, S., Green, P., Haywood, M., Kirton, L. G., . . . Somerfield, P. J. (2008). The habitat function of mangroves for terrestrial and marine fauna: A review. Aquatic Botany, 89(2), 155-185. doi: https://doi.org/10.1016/j.aquabot.2007.12.007

Nex, F., & Remondino, F. (2014). UAV for 3D mapping applications: A review. Applied Geomatics, 6. doi: https://doi.org/10.1007/s12518-013-0120-x

Ngo, D., Nguyen, H., Dang, C., & Kolesnikov, S. (2020). UAV application for assessing rainforest structure in Ngoc Linh nature reserve, Vietnam. E3S Web Conf., 203, 03006.

Nguyen, D. H., & Ngo, T. D. (2021). Seasonal Dynamics of Tropical Forest Vegetation in Ngoc Linh Nature Reserve, Vietnam Based on UAV Data. Forest and Society, 5(2), 376-389. doi: https://doi.org/10.24259/fs.v5i2.13027

Nguyen, D. H., Ngo, T. D., Vu, V. D., & Du, Q. V. V. (2022). Establishing distribution maps and structural analysis of seagrass communities based on high-resolution remote sensing images and field surveys: a case study at Nam Yet Island, Truong Sa Archipelago, Vietnam. Landscape and Ecological Engineering. doi: https://doi.org/10.1007/s11355-022-00502-0

Nguyen, H. H., Nghia, N. H., Nguyen, H. T. T., Le, A. T., Ngoc Tran, L. T., Duong, L. V. K., . . . Furniss, M. J. (2020). Classification Methods for Mapping Mangrove Extents and Drivers of Change in Thanh Hoa Province, Vietnam during 2005-2018. Forest and Society, 4(1), 225-242. doi: 10.24259/fs.v4i1.9295

Nguyen, L. D., Nguyen, C. T., Le, H. S., & Tran, B. Q. (2019). Mangrove Mapping and Above-Ground Biomass Change Detection using Satellite Images in Coastal Areas of Thai Binh Province, Vietnam. Forest and Society, 3(2), 248-261. doi: 10.24259/fs.v3i2.7326

Nhan, H. T. T., Hai, H. T., & Canh, L. X. (2015). Biological deversity in Xuan Thuy National Park, Nam Dinh Province. Paper presented at the The 5th National Scientific Conference on Ecology and Biological Resources, Ha Noi.

Nicholls, R. (2004). Coastal Flooding and Wetland Loss in the 21st Century: Changes Under the SRES Climate and Socio-Economic Scenarios. Global Environmental Change, 14, 69-86. doi: 10.1016/j.gloenvcha.2003.10.007

Nur W, M., Hapsara, R., Cahyo, R., Wahyu, G., Syarif, A., Umarhadi, D., . . . Widyatmanti, W. (2017). Mangrove Structure Mapping Model Using Sentinel-2A Satellite Imagery. Paper presented at the International Symposium on Remote Sensing Japan.

Okojie, J. (2017). Assessment of the relative accuracy of canopy height models developed from UAV and LiDAR sourced datasets for forest tree height estimation in temperate forests. Paper presented at the Geospatial Systems for Apps Development and Research in Africa, Asokoro, Abuja.

Otero, V., Van De Kerchove, R., Satyanarayana, B., Martínez-Espinosa, C., Fisol, M. A. B., Ibrahim, M. R. B., . . . Dahdouh-Guebas, F. (2018). Managing mangrove forests from the sky: Forest inventory using field data and Unmanned Aerial Vehicle (UAV) imagery in the Matang Mangrove Forest Reserve, peninsular Malaysia. Forest Ecology and Management, 411, 35-45. doi: https://doi.org/10.1016/j.foreco.2017.12.049

Pal, S., Mishra, A., & Singh, P. (2020). Assessment of Normalized Difference Vegetation Index by The Use of UAV Remote Sensing. International Journal of Advanced Science and Technology, 29, 4907-4914.

Panagiotidis, D., Abdollahnejad, A., Surovy, P., & Chiteculo, V. (2018). High resolution airborne UAV imagery to determine tree height and crown diameter.

Pardo-Iguzquiza, E., Dowd, P., Ruiz-Constán, A., Martos-Rosillo, S., Luque-Espinar, J. A., Rodriguez-Galiano, V., & Pedrera, A. (2018). Epikarst mapping by remote sensing. Catena, 165, 1-11. doi: https://doi.org/10.1016/j.catena.2018.01.026

Pellegrini, J., Soares, M., Chaves, F., Estrada, G., & Cavalcanti, V. (2009). A Method for the Classification of Mangrove Forests and Sensitivity/Vulnerability Analysis. Journal of Coastal Research, SI56, 443-447.

People's Committee of Tien Yen district. (2015). General report on socio-economic development master plan of Tien Yen district to 2020, orientation to 2030. Quang Ninh.

Pham, T. D., Yoshino, K., & Kaida, N. (2017). Monitoring Mangrove Forest changes in Cat Ba Biosphere Reserve using ALOS PALSAR Imagery and a GIS-based Support Vector Machine Algorithm. Paper presented at the International Conference on Geo-Spatial Technologies and Earth Resource.

Polidoro, B., Carpenter, K., Collins, L., Duke, N., Ellison, A., Ellison, J., . . . Yong, J. (2010). The Loss of Species: Mangrove Extinction Risk and Geographic Areas of Global Concern. PloS one, 5, e10095. doi: https://doi.org/10.1371/journal.pone.0010095

Prasetyo, L., Nursal, W., Setiawan, Y., Rudianto, Y., Wikantika, K., & Irawan, B. (2019). Canopy cover of mangrove estimation based on airborne LIDAR & Landsat 8 OLI. IOP Conference Series: Earth and Environmental Science, 335, 012029. doi: 10.1088/1755-1315/335/1/012029

Prinzie, A., & Van den Poel, D. (2007). Random Multiclass Classification: Generalizing Random Forests to Random MNL and Random NB (Vol. 4653).

Qiao, L., Tang, W., Dehua, G., Zhao, R., An, L., Li, M., . . . Song, D. (2022). UAV-based chlorophyll content estimation by evaluating vegetation index responses under different crop coverages. Computers and Electronics in Agriculture, 196, 106775. doi: 10.1016/j.compag.2022.106775

Rhyma, P. P., Kamarudin, N., Omar, H., Faridah-Hanum, I., & Wahab, Z. (2019). Integration of normalised different vegetation index and Soil-Adjusted Vegetation Index for mangrove vegetation delineation. Remote Sensing Applications: Society and Environment, 17, 100280. doi: 10.1016/j.rsase.2019.100280

Richter, R., Reu, B., Wirth, C., Doktor, D., & Vohland, M. (2016). The use of airborne hyperspectral data for tree species classification in a species-rich Central European forest area. International Journal of Applied Earth Observation and Geoinformation, 52, 464-474. doi: 10.1016/j.jag.2016.07.018

Saenger, P. (2002). Mangrove Structure and Classification (pp. 183-205).

Safford, R. J., Tran, T., Maltby, E., & Ni, D. (1998). Status, biodiversity and management of the U Minh wetlands, Vietnam. Tropical Biodiversity, 5, 217-244.

Samsuri, S., Zaitunah, A., Meliani, S., Hasnanda Syahputra, O., Budiharta, S., Susilowati, A., . . . Azhar, I. (2021). Mapping of mangrove forest tree density using SENTINEL 2A satelit image in remained natural mangrove forest of Sumatra eastern coastal. IOP Conference Series: Earth and Environmental Science, 912, 012001. doi: https://doi.org/10.1088/1755-1315/912/1/012001

Sarno, Rujito, A. S., Zulkifli, D., Munandar, & Moh. Rasyid, R. (2015). Primary Mangrove Forest Structure and Biodiversity. Int J Agri Sys, 2, 135–141. doi: http://dx.doi.org/10.20956/ijas.v3i2.102

Singgalen, Y. (2022). Vegetation Index and Mangrove Forest Utilization through Ecotourism Development in Dodola and Guraping of North Maluku Province. Jurnal Manajemen Hutan Tropika (Journal of Tropical Forest Management), 28, 150-161. doi: https://doi.org/10.7226/jtfm.28.2.150

Singgalen, Y., Gudiato, C., Prasetyo, S., & Fibriani, C. (2021). Mangrove monitoring using normalized difference vegetation index (NDVI): case study in North Halmahera, Indonesia. Jurnal Ilmu dan Teknologi Kelautan Tropis, 13, 2. doi: https://doi.org/10.29244/jitkt.v13i2.34771

Song, B., & Park. (2020). Detection of Aquatic Plants Using Multispectral UAV Imagery and Vegetation Index. Remote Sensing, 12, 387. doi: 10.3390/rs12030387

Thinh, N., Huan, N., Pham, U., & Sơn Tùng, N. (2008). Landscape ecological planning based on change analysis: A case study of mangrove restoration in Phu Long-Gia Luan area, Cat Ba Archipelago. VNU Journal of Science, Earth Sciences, 24, 133-144.

Tiwari, A., Sharma, S., Dixit, A., & Mishra, V. (2020). UAV Remote Sensing for Campus Monitoring: A Comparative Evaluation of Nearest Neighbor and Rule-Based Classification. Journal of the Indian Society of Remote Sensing, 49. doi: https://doi.org/10.1007/s12524-020-01268-4

Toan, D. (2014). Statistical assessment of the properties of the East Sea and the coast of Vietnam in the period 1951-2013. Estuarine and Coastal Marine Science, 12, 13.

Tucker, C. (1979). Red and Photographic Infrared Linear Combinations for Monitoring Vegetation. Remote Sensing of Environment, 8. doi: https://doi.org/10.1016/0034-4257(79)90013-0

Van, T., Nguyen Dang, M., Khiem, M., Duong, T. H., Van, K., Thanh, T., . . . Minh, T. (2022). Climatic Factors Associated with Heavy Rainfall in Northern Vietnam in Boreal Spring. Advances in Meteorology, 2022, 1-14. doi: https://doi.org/10.1155/2022/5917729

Viet, H., Potokin, A., Anh, D., Nguyen, T., & Nguyen, T. (2020). Forest Vegetation Cover in Tram Chim National Park in Southern Vietnam. IOP Conference Series: Earth and Environmental Science, 574, 012014. doi: https://doi.org/10.1088/1755-1315/574/1/012014

Watson, J. (1925). Mangrove Forests of the Malay Peninsula. Malays. For. Rec., 6, 1-275.

Xue, L., & Yang, L. (2009). Deriving leaf chlorophyll content of green-leafy vegetables from hyperspectral reflectance. Isprs Journal of Photogrammetry and Remote Sensing - ISPRS J PHOTOGRAMM, 64, 97-106. doi: 10.1016/j.isprsjprs.2008.06.002

Yaney-Keller, A., Tomillo, P., Marshall, J., & Paladino, F. (2019). Using Unmanned Aerial Systems (UAS) to assay mangrove estuaries on the Pacific coast of Costa Rica. PloS one, 14, e0217310. doi: 10.1371/journal.pone.0217310

Yeom, J., Jung, J., Chang, A., Ashapure, A., Maeda, M., Maeda, A., & Landivar, J. (2019). Comparison of Vegetation Indices Derived from UAV Data for Differentiation of Tillage Effects in Agriculture. Remote Sensing, 11, 1548. doi: 10.3390/rs11131548

Yin, D., & Wang, L. (2019). Individual mangrove tree measurement using UAV-based LiDAR data: Possibilities and challenges. Remote Sensing of Environment, 223, 34-49. doi: 10.1016/j.rse.2018.12.034

Yunjun, Y., Deng, H., Liu, Y., & Zhu. (2019). Application of UAV-Based Multi-Angle Hyperspectral Remote Sensing in Fine Vegetation Classification. Remote Sensing, 11, 2753. doi: https://doi.org/10.3390/rs11232753

Zahra, N., Setiawan, Y., & Prasetyo, L. (2022). Estimation of Mangrove Canopy Cover Using Unmanned Aerial Vehicle (UAV) in Indramayu Regency, West Java. IOP Conference Series: Earth and Environmental Science, 950, 012032. doi: 10.1088/1755-1315/950/1/012032

Zhang, C. (2020). Assessing the Effects of Hurricane Irma on Mangrove Structures in the Coastal Everglades using Airborne Lidar Data Multi-sensor System Applications in the Everglades Ecosystem (1st Edition ed., pp. 289-302).

Zhao, Y., Yan, C., Lu, S., Wang, P., Qiu, G., & Li, R. (2019). Estimation of chlorophyll content in intertidal mangrove leaves with different thicknesses using hyperspectral data. Ecological Indicators, 106, 105511. doi: 10.1016/j.ecolind.2019.105511

Zulfa, A. W., Norizah, K., Hamdan, O., Faridah-Hanum, I., Rhyma, P. P., & Fitrianto, A. (2021). Spectral signature analysis to determine mangrove species delineation structured by anthropogenic effects. Ecological Indicators, 130, 108148. doi: https://doi.org/10.1016/j.ecolind.2021.108148

Zulfa, A. W., Norizah, K., Hamdan, O., Zulkifly, S., Faridah-Hanum, I., & Rhyma, P. P. (2020). Discriminating trees species from the relationship between spectral reflectance and chlorophyll contents of mangrove forest in Malaysia. Ecological Indicators, 111, 106024. doi: https://doi.org/10.1016/j.ecolind.2019.106024